[5]J. Güémez and S. Velasco, "A probabilistic method to calculate the probability distribution of a gas," Eur. J. Phys. **8**, 75–80 (1987).
[6]F. Reif, *Fundamentals of Statistical and Thermal Physics* (McGraw-Hill, New York, 1965), pp. 426–427.
[7]K. G. Wilson, "Problems in physics with many scales of length," Sci. Am. **241**, 140–157 (1979).
[8]P. G. de Gennes, "Fluctuations géantes et phénomènes critiques," La Recherche **5** (51), 1022–1031 (1974).
[9]J. Güémez, S. Velasco, and A. Calvo Hernàndez, "Probability distribution for a lattice gas model. I. General study," Physica A **152**, 226–242 (1988).
[10]J. Güémez, S. Velasco, and A. Calvo Hernàndez, "Probability distribution for a lattice gas model. II. Thermodynamic limit," Physica A **152**, 243–253 (1988).
[11]J. M. Pimbley, "Volume exclusion correction to the ideal gas with a lattice gas model," Am. J. Phys. **54**, 54–57 (1986).
[12]P. T. Landsberg, *Problems in Thermodynamics and Statistical Physics* (Pion, London, 1971), pp. 252–253.

The solution of the Dirac equation for a high square barrier

Mark J. Thomson[a] and Bruce H. J. McKellar
Research Centre for High Energy Physics, School of Physics, Melbourne University, Parkville 3052, Australia

(Received 2 December 1988; accepted for publication 24 August 1990)

The transmission of a Dirac particle through a high ($V_0 > E + m$) square electrostatic potential barrier is investigated further. As is well known, the transmission coefficient is nonzero even as V_0 goes to infinity. As well as reproducing the usual wave mechanics approach, a detailed fermion–antifermion multiple scattering calculation and an S-matrix calculation are examined to provide additional insight into the problem. The origin of the curious behavior is found to be the result of pair creation and annihilation events.

I. INTRODUCTION

The Klein paradox[1] is one of the most interesting one-particle relativistic wave mechanics problems; its resolution is both informative and beautiful. With the benefit of hindsight we can see that it foreshadowed the process of pair production which is more usually associated with second quantized relativistic field theories. In some sense, it provides a plausible link between the usual one-particle results and the now familiar field theory results. It is natural, then, that consideration of the Klein paradox is a valuable exercise for beginning students of relativistic quantum theory.

In this paper we present another one-particle relativistic wave mechanics problem that introduces not only the process of pair creation but also of pair annihilation. The transmission and reflection coefficients for a fermion incident upon an electrostatic square barrier of height V_0, where $V_0 > E + m$, are calculated by a variety of different methods.

The calculations are done in parallel to previously established results concerning the Klein paradox. As will be shown, the key to understanding the problem is the careful introduction of pair creation and annihilation events.

II. RELATIVISTIC FERMIONS IN STRONG POTENTIALS

We begin by considering the one-dimensional Dirac equation for a fermion in an electrostatic field,

$$(E - V_0)\Psi(x) + i\alpha_x \frac{\partial}{\partial x}\Psi(x) - \beta m \Psi(x) = 0. \quad (1)$$

$\Psi(x)$ is a two-spinor wave function and α_x, β are two 2×2 anticommuting Hermitian unitary matrices (in one space and one time dimension the Dirac algebra can be realized on 2×2 matrices). A convenient representation for these matrices, in terms of the Pauli matrices, is

$$\alpha_x = \sigma_x, \quad \beta = \sigma_z. \quad (2)$$

Confining our attention to systems containing regions of constant potential V_0 and regions of zero potential, we find the following sets of linearly independent normalized solutions for each region. For regions in which $V_0(x) = 0$, we have

$$\psi^R = N_k \begin{pmatrix} 1 \\ \lambda \end{pmatrix} e^{ikx}, \quad (3)$$

$$\psi^L = N_k \begin{pmatrix} 1 \\ -\lambda \end{pmatrix} e^{-ikx}, \quad (4)$$

where

$$k^2 = E^2 - m^2, \quad (5)$$

$$\lambda = k/(E + m), \quad (6)$$

$$N_k^2 = [1/(1 + \lambda^2)](1/2\pi), \quad (7)$$

and for regions in which $V(x) = V_0$,

$$\Psi^R = N_K \begin{pmatrix} 1 \\ \Lambda \end{pmatrix} e^{iKx}, \quad (8)$$

$$\Psi^L = N_K \begin{pmatrix} 1 \\ -\Lambda \end{pmatrix} e^{-iKx}, \quad (9)$$

where

$$K^2 = (E - V_0)^2 - m^2, \quad (10)$$

$$\Lambda = K/(E - V_0 + m), \quad (11)$$

$$N_K^2 = [1/(1 + \Lambda^2)](1/2\pi). \quad (12)$$

In both cases, the above eigenstates are normalized on the

assumption that they extend over the whole line, that is, integration from minus to plus infinity in x of $\Psi_{k'}^{\dagger}\Psi_k$ gives $\delta(k'-k)$. Strictly speaking, the normalization is unimportant because we shall only be interested in the ratios of currents. Nevertheless, we have included the normalization to conform with the usual representation of the eigenstates.

In what follows, we shall be concerned exclusively with values of V_0 such that $V_0 > E + m$. In this case, both k and K are real and the above states are plane-wave solutions. The superscript R (L) indicates that the eigenvalue of momentum is $+K$ or $+k$ ($-K$ or $-k$), as appropriate.

The general solution in a region of zero potential is

$$\psi_n = a_n \psi^R + b_n \psi^L, \tag{13}$$

where the subscript n indexes the region and $|a_n|^2 + |b_n|^2 = 1$ to ensure normalization. Similarly, for a region of constant potential V_0, we find that

$$\Psi_m = A_m \Psi^R + B_m \Psi^L, \tag{14}$$

where once again m is a region index and $|A_m|^2 + |B_m|^2 = 1$.

The solution to a given problem will be given by matching the general solutions with the appropriate boundary conditions and by demanding overall continuity of the wave function. The algebra can be simplified by introducing matching matrices[2] that relate a_n, b_n to $A_{n\pm1}, B_{n\pm1}$, the coefficients in adjacent regions.

Consider the boundary at point x_0 between a region of potential V_0 and a region of zero potential, the coefficients a_n, b_n are related to $A_{n\pm1}$, $B_{n\pm1}$ by

$$\begin{pmatrix} a_n \\ b_n \end{pmatrix} = M(x_0)\begin{pmatrix} A_{n\pm1} \\ B_{n\pm1} \end{pmatrix}, \tag{15}$$

$$\begin{pmatrix} A_{n\pm1} \\ B_{n\pm1} \end{pmatrix} = M(x_0)^{-1}\begin{pmatrix} a_n \\ b_n \end{pmatrix}, \tag{16}$$

where

$$M(x_0) = \frac{N_K}{2N_k}\begin{pmatrix} (1+\Lambda/\lambda)e^{i(K-k)x_0} & (1-\Lambda/\lambda)e^{-i(K+k)x_0} \\ (1-\Lambda/\lambda)e^{i(K+k)x_0} & (1+\Lambda/\lambda)e^{-i(K-k)x_0} \end{pmatrix}. \tag{17}$$

In this manner the wave function is guaranteed to be continuous at all points.

We are now ready to look at the systems of interest, the step potential and the square barrier.

III. THE STEP POTENTIAL, KLEIN PARADOX

Consider the potential

$$\begin{aligned} V(x) &= 0, \quad x<0, \quad \text{region I}, \\ &= V_0, \quad x>0, \quad \text{region II}, \end{aligned} \tag{18}$$

where $V_0 > E + m$. The solution in region I will be of the form (13) and the solution in the region II will be of the form (14). Thus a fermion of energy E is described by a wave function of the form

$$\begin{aligned} \psi &= a_{\rm I}\psi_{\rm I}^R + b_{\rm I}\psi_{\rm I}^L, \quad x<0 \\ &= A_{\rm II}\Psi_{\rm II}^R + B_{\rm II}\Psi_{\rm II}^L, \quad x>0. \end{aligned} \tag{19}$$

Klein[1] investigated the reflection and transmission by the step potential of a plane wave incident from the left with energy E. The boundary condition is $B_{\rm II} = 0$ corresponding to no particles incident from the right. For a wave function of the form (19), the current can be calculated using

$$j(x) = \Psi^+(x)\alpha_x\Psi(x), \tag{20}$$

yielding

$$\begin{aligned} j_{\rm I}(x) &= (k/E)(|a_{\rm I}|^2 - |b_{\rm I}|^2) \\ &= j_{\rm I}^R - j_{\rm I}^L, \quad x<0, \end{aligned} \tag{21}$$

$$\begin{aligned} j_{\rm II}(x) &= [K/(E-V_0)](|A_{\rm II}|^2 - |B_{\rm II}|^2) \\ &= j_{\rm II}^R - j_{\rm II}^L, \quad x>0. \end{aligned} \tag{22}$$

By substituting $x_0 = 0$ into (17) and then using (16) it is possible to calculate ratios of currents so as to determine reflection and transmission coefficients. It follows that

$$R = j_{\rm I}^L/j_{\rm I}^R = (1-\lambda/\Lambda)^2/(1+\lambda/\Lambda)^2, \tag{23}$$

$$T = j_{\rm II}^R/j_{\rm I}^R = 4(\lambda/\Lambda)/(1+\lambda/\Lambda)^2. \tag{24}$$

A paradox is immediately apparent, traveling wave solutions exist in a region in which the potential is greater than the energy of the particle. Nonrelativistic quantum mechanics predicts an exponentially decaying solution in such a case.[3] As the potential is increased toward infinity the nonrelativistic solution vanishes in the high-potential region but the relativistic solution does not. In fact, the reflection and transmission coefficients approach the constant values,

$$\lim_{V_0\to\infty} R = (1+\lambda)^2/(1-\lambda)^2, \tag{25}$$

$$\lim_{V_0\to\infty} T = -4\lambda/(1-\lambda)^2. \tag{26}$$

Furthermore, since λ is positive $R>1$ and $T<0$ which makes no sense from a classical viewpoint.

This anomalous result is consistent with the relationship between the magnitudes of the currents flowing into and out of the barrier

$$|j_{\rm I}^L| = |j_{\rm I}^R| + |j_{\rm II}^R|. \tag{27}$$

This can easily be shown by using (23) and (24). Thus the reflected current is equal in magnitude to the sum of the incident and transmitted current magnitudes. As we shall see, pair production at the barrier is responsible for this anomalous result.

IV. THE SQUARE BARRIER

Consider the potential

$$\begin{aligned} V(x) &= 0, \quad x<0, \quad \text{region I} \\ &= V_0, \quad 0<x<a, \quad \text{region II} \\ &= 0, \quad a<x, \quad \text{region III}. \end{aligned} \tag{28}$$

The solution will be of the form

$$\begin{aligned} \psi &= a_{\rm I}\psi_{\rm I}^R + b_{\rm I}\psi_{\rm I}^L, \quad x<0, \\ &= A_{\rm II}\Psi_{\rm II}^R + B_{\rm II}\Psi_{\rm II}^L, \quad 0<x<a, \\ &= a_{\rm III}\psi_{\rm III}^R + b_{\rm III}\psi_{\rm III}^L, \quad a<x. \end{aligned} \tag{29}$$

Once again, we consider the reflection and transmission of a fermion of energy E incident from the left. The boundary condition is $b_{\rm III} = 0$, that is, no particles are incident from the right. Using the appropriate matching matrices at $x_0 = 0$ and $x_0 = a$, the reflection and transmission coeffi-

cients can be calculated[2] just as in Sec. III. We find

$$T=\frac{j_{\mathrm{III}}^{R}}{j_{\mathrm{I}}^{R}}=\frac{1}{1+\frac{1}{4}\left(\Lambda/\lambda-\lambda/\Lambda\right)^{2}\sin^{2}(Ka)}, \tag{30}$$

$$R=\frac{j_{\mathrm{I}}^{L}}{j_{\mathrm{I}}^{R}}=\frac{\frac{1}{4}\left(\Lambda/\lambda-\lambda/\Lambda\right)^{2}\sin^{2}(Ka)}{1+\frac{1}{4}\left(\Lambda/\lambda-\lambda/\Lambda\right)^{2}\sin^{2}(Ka)}. \tag{31}$$

Unlike the reflection and transmission coefficients for the step potential (30) and (31) are both positive and in the range [0,1]. By inspection $T+R=1$, as would be expected by particle conservation considerations. Although the square barrier fails to exhibit all the anomalous behavior that occurred with the step potential, it is nonetheless paradoxical. In the limit $V_0\to\infty$, we find

$$\lim_{V_0\to\infty} T=\frac{1}{1+\frac{1}{4}\left(\lambda-1/\lambda\right)^{2}\sin^{2}(Ka)}, \tag{32}$$

$$\lim_{V_0\to\infty} R=\frac{\frac{1}{4}\left(\lambda-1/\lambda\right)^{2}\sin^{2}(Ka)}{1+\frac{1}{4}\left(\lambda-1/\lambda\right)^{2}\sin^{2}(Ka)}. \tag{33}$$

Thus, even as the potential goes to infinity, the probability of particle transmission remains nonzero as for the step potential; this contradicts the intuition based on the nonrelativistic Schrödinger equation result. As we shall see, a single model will provide a consistent explanation of both the step potential and the square potential systems, and assists us in developing an intuitive picture of the physics of the relativistic barrier problem.

V. MULTIPLE SCATTERING APPROACH

The aim of this section will be to develop a model that explains qualitatively and predicts quantitatively the results of the previous sections. Ultimately, the model will be found to be simple and straightforward although it will combine aspects of first and second quantization of the Dirac field. The key to understanding the behavior of both the step potential and the square barrier is the interpretation of the traveling wave solutions in the regions of high potential.

We begin by examining Greiner's discussion of the Klein paradox.[4] Consider the positive and negative energy solutions of Dirac's equation, a continuum of free-particle states exists for $E\geqslant m$ and $E\leqslant -m$ as shown in Fig. 1(a).

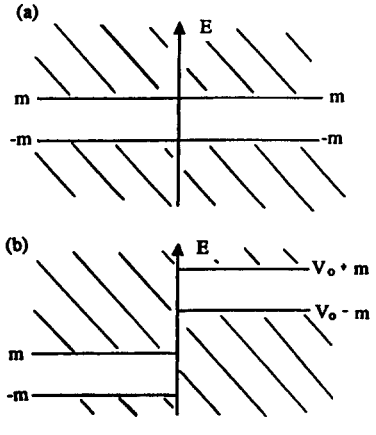

Fig. 1. (a) A schematic representation of the positive and negative energy continuum energy levels for a free fermion. (b) The same, but for a fermion in the presence of a strong field.

When an external electrostatic step potential is applied the situation is as shown in Fig. 1(b), particles of energy $E<V_0+m$ impinge upon the already occupied Dirac sea of negative energy states. Greiner explains the Klein paradox qualitatively by proposing that the incident fermion "knocks out" an electron from the Dirac sea and a hole in the sea then propagates away to the right. The hole is, of course, an antifermion and corresponds to a traveling wave solution of the Dirac equation with $V_0>E+m$.

Further, let us examine the expression for the current in a region of potential $V_0(V_0>E+m)$,

$$j(x)=K/(E-V_0)(|A|^2-|B|^2). \tag{34}$$

The first (second) term corresponds to the current associated with plane waves having momentum eigenvalue $K(-K)$. Since $(E-V_0)<0$ the current in each case is in the opposite direction to the momentum. As before, the proposal is that these are antifermion states, the opposite sign of the current coming from the opposite charge which the antifermion carries. We henceforth adopt the following interpretation, $\Psi^R(\Psi^L)$ is the wave function of an antifermion moving to the right (left).

Hansen and Ravndal[5] use a similar interpretation in their discussion of the Klein paradox. In what follows we build upon Hansen and Ravndals' resolution of the Klein paradox by producing a model for the transmission and reflection of fermions by a square barrier.

Having settled upon an interpretation of the wave functions in regions of high potential, we now consider the possible events that can occur between a region of high potential and a region of zero potential, that is, processes that can occur at the interface between a region of fermions and a region of antifermions. Four possible events can proceed: they are pair production, pair annihilation, fermion reflection, and antifermion reflection. They are depicted in Fig. 2.

The reflection and transmission by the step and square potentials can be understood in terms of events involving combinations of the four basic processes (Fig. 2).

In the case of the step potential, only two possible processes are compatible with the boundary conditions, fermion reflection and pair production. These are shown diagrammatically in Fig. 3.

Before proceeding any further, we note that Fig. 3 predicts correctly the relationship between the magnitudes of the currents involved (27). The reflected current is equal in magnitude to the magnitudes of the incident and transmitted currents together.

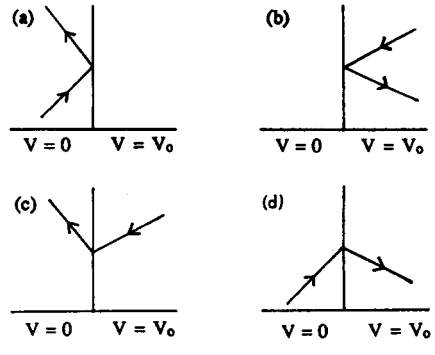

Fig. 2. The diagrammatic representation of (a) fermion reflection; (b) antifermion reflection; (c) pair production; and (d) pair annihilation.

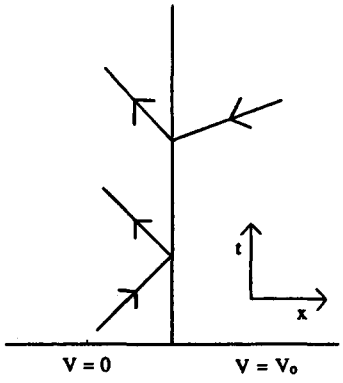

Fig. 3. The diagrammatic representation of the fundamental processes that occur in the step potential problem.

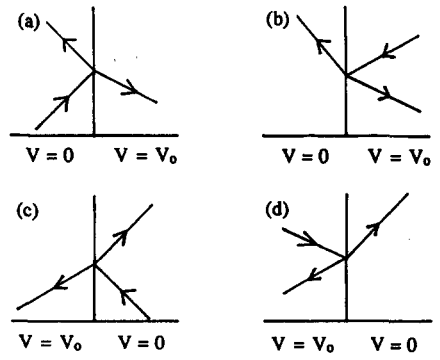

Fig. 4. The diagrams representing a fermion traveling forward [(a) and (c)] and backward [(b) and (d)] in time which impinges upon an interface.

Consider now the Feynman interpretation of antifermions.[6] An antifermion traveling forward in time is interpreted as a fermion traveling backward in time. This viewpoint leads us to consider a fermion (an antifermion) incident on the interface with a region of high (zero) potential. The diagrams for such events are shown in Fig. 4.

Thus a fermion traveling forward in time is either scattered backward in time (pair annihilation) or reflected elastically by the interface. Similarly, a fermion traveling backward in time is either scattered forward in time (pair production) or reflected elastically.

The wave functions for the four systems (Fig. 4) are easily calculated using the techniques of Sec. I. The wave function in the region of a step potential is a linear combination of Fig. 4(a) and 4(c) such that the boundary condition $B_{II} = 0$ is satisfied.

Let Ψ_α be the wave function of the diagram shown in Fig. 4(α) for $\alpha = a,b,c,d$. Then

$$\psi_a = a_a\psi^R + b_a\psi^L, \quad x < x_0,$$
$$= B_a\Psi^L, \quad x > x_0. \tag{35}$$
$$\psi_b = A_b\Psi^R, \quad x < x_0,$$
$$= a_b\psi^R + b_b\psi^L, \quad x > x_0, \tag{36}$$
$$\psi_c = b_c\psi^L, \quad x < x_0,$$
$$= A_c\Psi^R + B_c\Psi^L, \quad x > x_0, \tag{37}$$
$$\psi_d = A_d\Psi^R + B_d\Psi^L, \quad x < x_0,$$
$$= a_d\psi^R, \quad x > x_0. \tag{38}$$

Having exhausted the possible barrier–particle interactions, we can now employ the multiple scattering expansion[7,8] to determine the overall scattering properties of the square barrier. The analogous Schrödinger equation problem has already been dealt with in this fashion by Anderson.[7] The Dirac equation problem is somewhat more picturesque because of the introduction of pair annihilation and creation events.

We now define amplitude reflection and transmission coefficients as follows. The amplitude reflection coefficient is the ratio of the reflected fermion (antifermion) amplitude to the incident fermion (antifermion) amplitude. Similarly, the amplitude transmission coefficient is the ratio of the outgoing fermion (antifermion) amplitude to the incident antifermion (fermion) amplitude. Following this definition the amplitude reflection and transmission coefficients for the processes shown in Fig. 4 are

$$R_a = b_a/a_a = M_{22}(x_0)/M_{12}(x_0),$$
fermion reflection, (39)
$$T_a = B_a/a_a = 1/M_{12}(x_0),$$
pair annihilation/transmission, (40)
$$R_b = a_b/b_b = M_{11}(x_0)/M_{21}(x_0),$$
fermion reflection, (41)
$$T_b = A_b/b_b = 1/M_{21}(x_0),$$
pair annihilation/transmission, (42)
$$R_c = B_c/A_c = M_{22}(x_0)^{-1}/M_{12}(x_0)^{-1},$$
antifermion reflection, (43)
$$T_c = b_c/A_c = 1/M_{12}(x_0)^{-1},$$
pair production/transmission, (44)
$$R_d = A_d/B_d = M_{11}(x_0)^{-1}/M_{21}(x_0)^{-1},$$
antifermion reflection, (45)
$$T_d = a_d/B_d = 1/M_{21}(x_0)^{-1},$$
pair production/transmission. (46)

R_α, T_α are, in general, complex numbers unlike the true probability reflection and transmission coefficients that are real. The total amplitude is the sum of all the amplitudes corresponding to possible fermion paths through the system. Each individual path contributes an amplitude calculated by considering the reflection and transmission incurred at each interface.

For example, a fermion incident from the right with amplitude A_0, which is refracted backward in time by an interface at $x = x_0$, will have an amplitude $T_a(x_0)A_0$. Likewise, a fermion incident from the right, which is reflected elastically, will have amplitude $R_a(x_0)A_0$. In this manner, we can calculate the contribution to the amplitude for a particular event by any given fermion path.

Specifically, the reflection or transmission of a fermion by a square barrier can be depicted diagrammatically by an infinite number of possible paths. Each of these paths can be thought of as the scattering of a single fermion by a sequence of the fundamental processes of Fig. 2. The diagrams that represent the paths for these various amplitudes are shown in Fig. 5.

The amplitude for a fermion path resulting in transmission through the barrier after n reflections $A_T^{(n)}$ can be

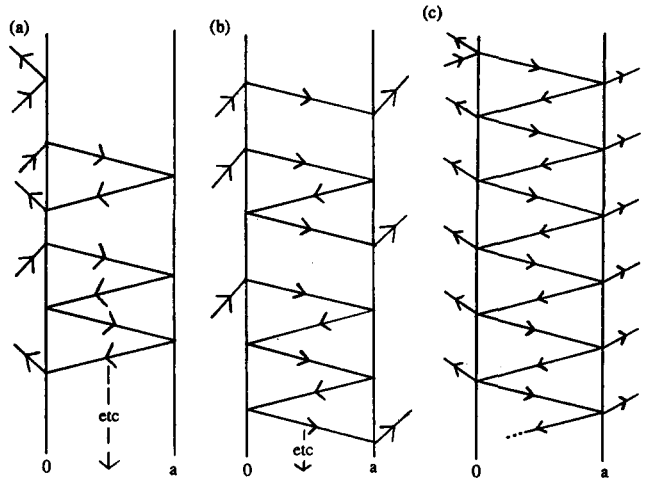

Fig. 5. (a) Diagrams representing reflection; (b) transmission; (c) the diagrammatic sum of (a) and (b), which can be thought of as the diagram representing the wave function of the system.

found using (39) through (46),

$$A_T^{(n)} = T_a(0)T_d(a)R_c^n(0)R_d^n(a)A_0, \tag{47}$$

where A_0 is the initial amplitude and n is half the number of reflections that occur. Similarly, the amplitude for a path corresponding to the reflection of a fermion after n reflections at the step at $x = a$ is

$$\begin{aligned} A_R^{(n)} &= R_a(0), n = 0, \\ &= T_a(0)T_c(0)R_c^{n-1}R_d^n(a), n \geqslant 1. \end{aligned} \tag{48}$$

The total amplitudes for reflection and transmission are found by summing the amplitudes corresponding to each path consistent with the appropriate endpoint. Thus

$$\begin{aligned} A_T &= \sum_{n=0} A_T(n) \\ &= A_0T_a(0)T_d(a)\sum_{n=0}[R_c(0)R_d(a)]^n \\ &= A_0T_a(0)T_d(a)[1 - R_c(0)R_d(a)]^{-1}, \end{aligned} \tag{49}$$

$$\begin{aligned} A_R = \sum_{n=0} A_R(n) &= A_0R_a(0) + A_0T_a(0)T_c(0) \\ &\quad \times \sum_{n=1} R_c^{n-1}(0)R_d^n(a) \\ &= A_0R_a(0)T_a(0)T_c(0)R_d(a) \\ &\quad \times [1 - R_c(0)R_d(a)]^{-1}. \end{aligned} \tag{50}$$

Substitution from (39) through (46) yields

$$\frac{A_R}{A_0} = \frac{(i/2)(\Lambda/\lambda - \lambda/\Lambda)\sin(Ka)}{\cos(Ka) - (i/2)(\Lambda/\lambda + \lambda/\Lambda)\sin(Ka)}, \tag{51}$$

$$\frac{A_T}{A_0} = \frac{1}{\cos(Ka) + (i/2)(\Lambda/\lambda + \lambda/\Lambda)\sin(Ka)}. \tag{52}$$

The absolute value of Eqs. (51), (52) yields the reflection (transmission) coefficient for the square barrier. Comparison with any standard optics text[9] reveals that the above calculation is simply the Fabry–Perot interferometer problem. Both the method of solution and the final results are the same. This demonstrates the close physical basis shared by some methods in optics and the multiple scattering expansion.

Thus the fermion–antifermion model in conjunction with the multiple scattering expansion is able to reproduce the quantitative results derived earlier. The advantage of this approach is that it introduces explicitly pair creation and annihilation so that a physical picture of the phenomena can be developed that explains the apparently anomalous results.

It is worthwhile at this point to say something about the physical basis underlining the pair-production and annihilation events. The electrostatic square barrier gives rise to an electric field that is infinite at the two discontinuous potential interfaces and zero elsewhere. Heuristically this strong electric field can be expected to give rise to pair production. Any virtual fermion–antifermion pairs at the interfaces will be ripped apart by the electric field before recombination can occur. The localization of the pair-production events at the potential interfaces is consistent with this picture. Similar considerations arise in the development of a charge vacuum about a highly charged body.[4]

The production of fermion–antifermion pairs at the interfaces does not give rise to asymptotically detectable antifermions. The antifermions only provide a bridge across the barrier through which the probability amplitude flows. Once a pair is produced, the antifermions move into the barrier while the fermions move away, since the antifermions (fermions) are constrained to exist only inside (outside) the high potential region. Any antifermions created at, or reflected from, one edge of the barrier are repelled from it and are subsequently reflected or annihilated at the other edge; they do not escape the region of the barrier.

VI. THE *S*-MATRIX APPROACH

Hansen and Ravndal[6] utilized the in–out formalism to reveal explicitly the pair production associated with the Klein paradox. They defined asymptotically fermionic and antifermionic, incoming and outgoing solutions to the Dirac equation in the presence of a step potential. These sets of solutions were then used as modes with which a general field operator could be expanded in terms of using the appropriate creation and annihilation operators.

The overlap between the orthonormalized incoming and the outgoing solutions provided the transformation coefficients between the two sets of creation and annihilation operators. By taking appropriate matrix elements it was possible to calculate the pair-production rate associated with the step potential. As we shall see, this approach also reproduces the transmission and reflection coefficients for the square barrier.

We begin by constructing solutions that correspond asymptotically to either incoming or outgoing fermions. Using (4) through (12) and (29) we can construct incoming solutions

$$\psi_{\rm I}^{(\rm in)} = N_{\rm I}^{(\rm in)}(\psi_{\rm I}^R + a_{\rm II}\psi_{\rm II}^R + b_{\rm II}\psi_{\rm II}^L + a_{\rm III}\psi_{\rm III}^R + b_{\rm III}\psi_{\rm III}^L), \tag{53}$$

$$\psi_{\rm III}^{(\rm in)} = N_{\rm III}^{(\rm in)}(e_{\rm I}\psi_{\rm I}^R + f_{\rm I}\psi_{\rm I}^L + e_{\rm II}\psi_{\rm II}^R + f_{\rm II}\psi_{\rm II}^L + \psi_{\rm III}^L), \tag{54}$$

and outgoing solutions

$$\psi_{\rm I}^{(\rm out)} = N_{\rm I}^{(\rm out)}(\psi_{\rm I}^L + c_{\rm II}\psi_{\rm II}^R + d_{\rm II}\psi_{\rm II}^L + c_{\rm III}\psi_{\rm III}^R + d_{\rm III}\psi_{\rm III}^L), \tag{55}$$

$$\psi_{\rm III}^{(\rm out)} = N_{\rm III}^{(\rm out)}(g_{\rm I}\psi_{\rm I}^R + h_{\rm I}\psi_{\rm I}^L + g_{\rm II}\psi_{\rm II}^R + h_{\rm II}\psi_{\rm II}^L + \psi_{\rm III}^R). \tag{56}$$

It is understood that $\psi_{\rm I}^{L(R)}$ extends only over $x\leqslant 0$, $\psi_{\rm III}^{L(R)}$ extends only over $x\geqslant a$, and $\psi_{\rm II}^{L(R)}$ extends only over the interval $0\leqslant x\leqslant a$. The coefficients a, b, c, ..., h are determined by matching the solutions at the interfaces. The normalization factors $N_{\rm I}^{(\rm in)}$, $N_{\rm III}^{(\rm in)}$, $N_{\rm I}^{(\rm out)}$, and $N_{\rm III}^{(\rm out)}$ ensure that the solutions are normalized to delta functions in k space.

An arbitrary field operator can be expanded in either incoming or outgoing modes

$$\psi=\sum_k (a_{k,\rm I}^{(\rm in)}\psi_{k,\rm I}^{(\rm in)}+a_{k,\rm III}^{(\rm in)}\psi_{k,\rm III}^{(\rm in)}), \tag{57}$$

$$\psi=\sum_k (a_{k,\rm I}^{(\rm out)}\psi_{k,\rm I}^{(\rm out)}+a_{k,\rm III}^{(\rm out)}\psi_{k,\rm III}^{(\rm out)}), \tag{58}$$

As usual, the expansion coefficients $a_{k,\rm I}^{(\rm in)}$... are annihilation operators for a fermion corresponding to the solution $\psi_{k,\rm I}^{(\rm in)}$. Note that the expansions do not include antifermion modes. This is because for the potential defined, the positive energy solutions are all asymptotically fermionic, as discussed in Sec. VI.

It is a straightforward matter to calculate the transformations between the incoming and outgoing operators. We find that

$$a_{k,\rm I}^{(\rm out)}=S_{11}a_{k,\rm I}^{(\rm in)}+S_{12}a_{k,\rm III}^{(\rm in)}, \tag{59}$$

$$a_{k,\rm III}^{(\rm out)}=S_{21}a_{k,\rm I}^{(\rm in)}+S_{22}a_{k,\rm III}^{(\rm in)}. \tag{60}$$

The explicit values of the S-matrix elements are given by

$$\langle\psi_{\rm I}^{(\rm out)}(k')|\psi_{\rm I}^{(\rm in)}(k)\rangle=S_{11}\,\delta(k-k'), \tag{61}$$

$$\langle\psi_{\rm III}^{(\rm out)}(k')|\psi_{\rm III}^{(\rm in)}(k)\rangle=S_{22}\,\delta(k-k'), \tag{62}$$

$$\langle\psi_{\rm I}^{(\rm out)}(k')|\psi_{\rm III}^{(\rm in)}(k)\rangle=S_{12}\,\delta(k-k'), \tag{63}$$

$$\langle\psi_{\rm III}^{(\rm out)}(k')|\psi_{\rm I}^{(\rm in)}(k)\rangle=S_{21}\,\delta(k-k'), \tag{64}$$

where

$$S_{11}=N^2 2\pi\left[\frac{1}{4}\left(\frac{\Lambda}{\lambda}-\frac{\lambda}{\Lambda}\right)\left(\frac{\Lambda}{\lambda}+\frac{\lambda}{\Lambda}\right)\sin^2(Ka)-\frac{i}{2}\left(\frac{\Lambda}{\lambda}-\frac{\lambda}{\Lambda}\right)\sin(Ka)\cos(Ka)\right], \tag{65}$$

$$S_{22}=S_{11}e^{-i2ka}, \tag{66}$$

$$S_{12}=N^2 2\pi\left[\cos(Ka)+\frac{i}{2}\left(\frac{\Lambda}{\lambda}+\frac{\lambda}{\Lambda}\right)\sin(Ka)\right], \tag{67}$$

$$S_{21}=S_{12}, \tag{68}$$

and

$$N^2=2\pi\left[1+\frac{1}{4}\left(\frac{\Lambda}{\lambda}-\frac{\lambda}{\Lambda}\right)^2\sin^2(Ka)\right]. \tag{69}$$

We have employed the notation $S_{\alpha\beta}$ for the transformation coefficients because they correspond to the S-matrix elements between the in-solutions and the out-solutions.

The algebra involved in the normalization of the wave functions and the calculation of the transformation coefficients is very long and complicated. The symbolic manipulation program REDUCE[10] was used to produce the above results.

The wave function of system with a fermion of momentum k ($-k$) incident from the left (right) can be expressed in second quantized form as $a_{k,\rm I}^{+(\rm in)}|0,\rm in\rangle$ ($a_{k,\rm III}^{+(\rm in)}|0,\rm in\rangle$), where $|0,\rm in\rangle$ is the vacuum in the incoming basis. The number operators for the outgoing states moving to the left and right with momentum $-k$ (k) are

$$n_{k,\rm I}^{(\rm out)}=a_{k,\rm I}^{+(\rm out)}a_{k,\rm I}^{(\rm out)} \tag{70}$$

and

$$n_{k,\rm III}^{(\rm out)}=a_{k,\rm III}^{+(\rm out)}a_{k,\rm III}^{(\rm out)}, \tag{71}$$

respectively.

The expected number of reflected (transmitted) fermions resulting from a fermion incident from the left will be equal to the expectation value of the operator $n_{k,\rm I}^{(\rm out)}$ ($n_{k,\rm III}^{(\rm out)}$) corresponding to the state $a_{k,\rm I}^{+(\rm in)}|0,\rm in\rangle$. It is easy to show using (59) and (60) that

$$\langle n_{k,\rm I}^{(\rm out)}\rangle=|S_{11}|^2\langle 0,\rm in|0,in\rangle, \tag{72}$$

$$\langle n_{k,\rm III}^{(\rm out)}\rangle=|S_{12}|^2\langle 0,\rm in|0,in\rangle. \tag{73}$$

The normalized expectation values $|S_{11}|^2$ and $|S_{12}|^2$ can be calculated using (65) and (67). Since the state in question is a one particle state, we immediately regain the previously calculated reflection and transmission coefficients.

When Hansen and Ravndal[5] used the in–out formalism to calculate the transformation coefficients between the in and out operators for the step potential, they were able to calculate the rate at which pair production proceeded at the interface. This is not possible in the present case because all the states, incoming and outgoing, are fermionic as $|x|$ goes to infinity. As a result, the transformations map creation (annihilation) operators into creation (annihilation) operators exclusively. Without mixing between the creation and annihilation operators (and the resultant inequivalence of the incoming and outgoing vacuua) no asymptotically detectable pair creation can be expected.

This is not in contradiction with the earlier discussion of pair creation and annihilation in the vicinity of the barrier. The S matrix relates distant past with distant future states (which correspond to large negative or positive x values); it cannot be expected to contain information concerning pair creation and annihilation events near the origin unless these give rise directly to asymptotically detectable fermion–antifermion pairs.

Physically it is easy to understand how pair creation can occur while no antifermions travel out to infinity. For every pair creation event that occurs, a pair annihilation event ensures that consumes the antifermion, as illustrated in Fig. 5.

VII. CONCLUSION

Three quite different approaches were employed to calculate the reflection and transmission coefficients for a fermion incident upon a square barrier. The various approaches are instructive exercises in the methods they each employ. In addition to this, they provide an understanding of the phenomena from a variety of viewpoints.

The first approach used the usual wave mechanics technology to derive the results. This approach is firmly grounded in a wealth of similar problems which nonrelativistic quantum mechanics deals with successfully. Unfortunately this analysis does not give any hint as to why the barrier continues to transmit particles even as the height of the barrier goes to infinity.

The multiple scattering expansion in conjunction with the fermion–antifermion model successfully explains qualitatively and predicts quantitatively the reflection and transmission coefficients. The calculation is the most explanatory of the three approaches, the graphical represen-

tation of the process being particularly revealing.

Finally, the S-matrix approach introduces the language of second quantization to describe the reflection and transmission coefficients in terms of the expectation value of the appropriate number operators.

The concepts of antifermion states, pair production, and pair annihilation are important physical ideas in any relativistic quantum mechanics course. We believe that a detailed discussion of these concepts in the simple physical situation of scattering from a square barrier will help the student obtain some physical intuition for these ideas.

[a] Permanent address as of October 1990: Department of Physics, Schuster Laboratory, The University of Manchester, Manchester M13 9PL, United Kingdom.

[1] O. Klein, "Die Reflexion von Elektronen an einem Potentialsprung nach der relativistichen Dynamik von Dirac," Z. Phys. **53**, 157–165 (1929).

[2] Bruce H. J. McKellar and G. J. Stephenson, Jr., "Relativistic quarks in one dimensional periodic structures," Phys. Rev. C **35**, 2262–2271 (1987).

[3] Albert Messiah, *Quantum Mechanics* (North-Holland, Amsterdam, 1958).

[4] Walter Greiner, Berndt Müller, Johann Rafelski, *Quantum Electrodynamics of Strong Fields* (Springer-Verlag, New York, 1985).

[5] Alex Hansen and Finn Ravndal, "Klein's paradox and its resolution," Phys. Scr. **23**, 1036–1042 (1981).

[6] R. P. Feynman, "The theory of the positron," Phys. Rev. **76**, 749–759 (1949).

[7] Arlen Anderson, "Multiple scattering approach to one-dimensional potential problems," Am. J. Phys. **57**, 230–235 (1989).

[8] Barry R. Holstein "Semiclassical treatment of the double well," Am. J. Phys. **56**, 338–345 (1988).

[9] B. B. Rossi, *Optics* (Addison-Wesley, Reading, MA, 1959).

[10] Rand Corporation, REDUCE *Users Manual* (Rand Corporation, New York, 1984).

An inexpensive gas effusion apparatus for the introductory laboratory

Joseph C. Amato and Roger E. Williams

Department of Physics and Astronomy, Colgate University, Hamilton, New York 13346

(Received 28 June 1989; accepted for publication 24 August 1990)

An inexpensive, easy to build gas effusion apparatus for measuring molecular velocities is described. The instrument features a liquid nitrogen cooled adsorption pump to replace more costly diffusion and rotary vacuum pumps. Low cost, low maintenance, and simplicity of operation render the experiment suitable for introductory physics students. A straightforward measurement consistently yields average velocities within 10% of the calculated values.

I. INTRODUCTION

Several years ago, the Colgate Physics Department initiated a major revision of its introductory curriculum by offering a one-semester course in modern physics *before* the traditional two-semester sequence in classical mechanics and electromagnetism.[1] This revision was made in response to shrinking class enrollments as well as to our perception that incoming students were inadequately prepared for the usual calculus-based introductory course. We reasoned that modern physics could be presented without the burden of calculus which accompanies Newton's laws, and that it more accurately conveys the flavor of contemporary physics. We hoped to offer our students a glimpse of the excitement and challenge of present-day activity, and thus motivate the regimen of study they would encounter in the remainder of their undergraduate physics curriculum.

The new modern physics course required us to design and implement an accompanying set of laboratory exercises appropriate to our first-semester freshman audience. The theme of the course was atoms: What is the physical evidence for the atomic theory of matter? Consistent with this theme and with the spirit of the course, we attempted to develop a set of experiments which, whenever possible, went beyond the mere demonstration of lecture materials to include an element of discovery or surprise, akin to real research. (This ingredient—the essence of our own fascination with physics—seems sadly lacking in most traditional physics lab exercises.) We wanted our labs to illustrate how simple macroscopic instrumentation, guided by a straightfoward sequence of reasoning, can be used to "see" beyond what is directly visible, i.e., to probe the microscopic world of atoms and molecules. We also had more practical concerns: Contrary to the apparatus used in many modern physics experiments, ours had to be sufficiently inexpensive to allow for multiple setups (one for every two students). Furthermore, we desired a *dramatic* lead-off activity that would pique student interest, underscore the course goals, and lend compelling support to the atomic hypothesis. The experiment described below has fulfilled these expectations admirably.

II. EXPERIMENT DESIGN

The gas effusion technique for measuring molecular velocities is certainly not a new one.[2,3] What we have done is to design an inexpensive, reliable, easy to use apparatus suitable for the introductory laboratory. The unique feature of our design is the replacement of costly diffusion and rotary pumps by a simple liquid nitrogen cooled adsorption pump. The latter provides very high pumping speeds in the 1- to 100-mT pressure range, as required for the measurement. Figures 1 and 2 illustrate the apparatus.

